Thermal performance of common bulk-fill cryogenic insulation materials in helium and hydrogen background gases

A M Swanger[1]

[1]NASA Kennedy Space Center, Cryogenics Test Laboratory, NASA-KSC, FL 32899 USA

Email: adam.m.swanger@nasa.gov

Abstract. Maritime shipping of vast quantities of liquid hydrogen (LH_2) will be necessary to facilitate a global hydrogen ecosystem; with some studies estimating volumes up to 172,000 m^3 for individual tanker ships, and requiring stationary storage tanks at terminals of 50,000 m^3 to 100,000 m^3—ten to fifteen times larger than the current largest tank, located at launch pad B at NASA Kennedy Space Center (KSC). Such a radical scale-up will push the boundary of traditional, vacuum-insulated tank designs. Hence, a potential need exists for non-vacuum solutions, which necessitates exploring the thermal performance of insulation materials in non-condensable background gases at LH_2 temperatures, namely helium and hydrogen. Testing of two bulk-fill insulation materials common to large LH_2 storage tanks, perlite and glass bubbles, in helium and hydrogen was recently conducted by the Cryogenics Test Laboratory at KSC using the CS100 liquid nitrogen boiloff calorimeter per the ASTM C1774 standard methodology. Effective thermal conductivity (k_e) and heat flux (q) results for each insulation/gas combination are presented across the full vacuum range, as well as thermal profiles through the insulation thickness between 78 K and 293 K.

1. Introduction

To-date, virtually every liquid hydrogen (LH_2) storage tank has been a vacuum-insulated design: double-walled, with insulation, either reflective multilayer insulation (MLI) or bulk-fill powder, employed within the annular space and evacuated [1]. This configuration not only provides sufficient thermal performance, but safety benefits as well as most gases will readily liquefy inside the annular space when exposed to the inner tank surface at LH_2 temperatures (~20 K), which can compromise performance and possibly even the mechanical integrity of the vessel.

NASA Kennedy Space Center (KSC) currently owns and operates the largest LH_2 storage tanks in the world at launch pad 39B in Florida. Two vessels—one built during the Apollo program in the 1960s and used throughout the Space Shuttle program (1981-2011), and the other newly constructed (2022) to support the Artemis program—have usable LH_2 volumes of 3,200 m^3 [2] and 4,700 m^3 [3] respectively, yielding a combined hydrogen storage capacity of roughly 560 metric tons. Similar in construction, both tanks are traditional, double-walled, vacuum-insulated, spheres, with bulk-fill powder insulation—perlite in the legacy tank, glass bubbles in the new tank—with inner/outer diameters of 18.7 m / 21.4 m (Apollo-era tank), and 21.8 m / 25.3 m (new tank), and field-erected (that is, they were constructed on-site).

Recently, hydrogen has seen strong investment globally due to the potential for it to be more climate-friendly alternative to traditional fuels, and the role LH_2 needs to play in this new ecosystem is taking shape: that is, as a primary transport medium for shipping huge quantities of

energy around the world. Akin to the role liquefied natural gas (LNG) plays in the current energy ecosystem, feeding a vast global hydrogen network will require transport of LH_2 in ocean-going tanker ships in unprecedented volumes. And to facilitate this enterprise will demand storage and distribution systems at shipping terminals of commensurate scales. Recent studies estimate volumes up to 172,000 m^3 for individual tanker ships, and stationary storage tanks at terminals of 50,000 m^3 to 100,000 m^3 [4,5]—ten to fifteen times larger than the current largest tank at KSC. At such scales, constructing traditional vacuum-insulated tanks becomes problematic or impossible, due primarily to the massive vacuum pressure loading on the outer tank as the dimeter increases [6]. Figure 1 presents the two LH_2 spheres currently at KSC, along with their scaled models, and a 100,000 m^3 version of similar design for reference.

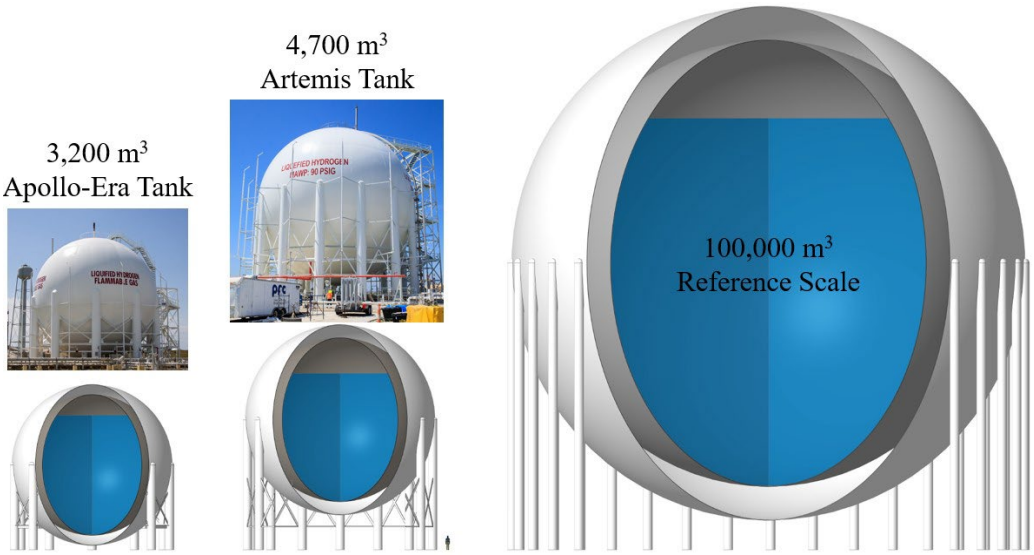

Figure 1. Scale Models of Both Existing LH_2 Spheres at Pad 39B at NASA-KSC, and a 100,000 m^3 Example Tank of Similar Design for Reference
(Note: Also for reference, the human placed beside the 4,700 m^3 tank is 1.85 m tall)

With much larger vacuum pressure loads comes an increase in tank wall thickness for strength. Eventually, practical and economic factors will win-out however, effectively rendering mega-scale designs infeasible, and as such, non-vacuum-insulated solutions may be necessary. However, as was previously mentioned, the choices of non-condensable background gases to fill the annular space are extremely limited. Helium is perhaps the most obvious option since the condensation point is well below that of LH_2, and it is inert. Unfortunately, economically, helium is problematic, and sustainability is always a concern due its non-renewable nature [7]. Hydrogen gas is the other viable option—and there would be an ample supply from normal liquid boiloff.

To the authors knowledge, neither helium nor hydrogen has ever been utilized as a background gas within the insulation space for cryogenic storage tanks. Aside from the very limited instances where either would need to be entertained for such an application, due to their properties, most notably their low densities and high thermal conductivities compared to more traditional purge gases such as nitrogen, there would undoubtedly be a substantial negative impact to the insulation performance. Poorer insulation performance leads to either higher boiloff for tanks of similar physical construction, or an increase in annular space thickness if a similar heat load is desired. Therefore, understanding the impact that helium and hydrogen background gas has on insulation performance is vital if non-vacuum-insulated tanks are to employ these options in future designs.

In 2022, the Cryogenics Test Laboratory (CTL) at KSC began characterizing the performance of two different common bulk-fill insulation materials, perlite and glass bubbles, used in large,

field-erected LH_2 tanks, in helium (99.995%) and hydrogen (99.9999%) background gases. Employing a standardized liquid nitrogen (LN_2) boiloff calorimeter, the CTL tested three different samples in both background gases, along with nitrogen (99.99%) as a baseline, over the full vacuum range. These examinations were undertaken in support of a US Department of Energy-funded effort led by Shell International Exploration & Production Inc. to develop a feasible LH_2 tank concept at a 100,000 m^3 scale [8]. And although the CTL testing would be limited to LN_2 temperature on the cold side (77 K), valuable data would nevertheless be obtained regarding the magnitude of the impact to insulation performance when employing the lighter gases. Data that could then be used to inform more sophisticated testing with LH_2 in the future, or to anchor predictive thermal models that could then be used to probe the LH_2 temperature range.

Effective thermal conductivity (k_e) and heat flux (q) results for each insulation/gas combination will be presented across the full vacuum range, as well as thermal profiles through the insulation thickness for temperatures between 78 K and 293 K.

2. Boiloff Calorimetry Test Setup

The CS100 instrument was used to perform testing on the bulk-fill powders. CS100 has been the flagship calorimeter of the CTL for over 20 years, and has successfully characterized a huge variety of insulation materials using a methodology formalized under ASTM C1774, Annex A1 [9].

A detailed description of the CS100 can be found in reference 10, but at a high level, the instrument is a vertical-cylindrical configuration, with a 1 m long × 167 mm diameter inner cold-mass assembly consisting of three independent LN_2 chambers sharing a common outer wall. An insulation specimen is oriented around the vertical pipe, and can be blankets, wraps, bulk-fill powder (with the aid of lower and outer containment barriers) or rigid clam-shell geometries, with an outer-most thin, aluminum heater sleeve to control the warm boundary temperature. The cold-mass assembly is suspended from a vacuum chamber lid, and with the aid of a custom lift, is removed/installed into a vacuum chamber for testing.

In the three-liquid-chamber configuration, the middle chamber is the test section, with upper and lower guard chambers to intercept any axial heat—this layout yields "absolute" k_e measurements, as the only heat being transmitted into the test chamber and causing boiloff is directed radially through the insulation (refer to ASTM C1774 for a more detailed explanation). Theses chambers are filled by-hand from portable LN_2 dewars, and once the process is complete the boiloff gas is routed to mass flow meters to the measure the flow rate. This flow rate is then paired with the heat of vaporization to determine the steady-state heat load in Watts, which is in turn linked to the effective thermal conductivity via the Fourier heat conduction equation.

The baseline CS100 design used an insulation thickness of 25 mm. However, due to the expected increase in heat flow rate from using helium and hydrogen background gases, that thickness was increased to 80.8 mm by using the heater sleeve as the outer containment for the bulk-fill powder. This additional thickness also allowed for a radial temperature rake assembly to aid in determining steady-state conditions as well as the thermal profile. A rake with seven type-E thermocouples, separated into roughly 10.1 mm layer increments by foam stand-offs, was positioned to measure the thermal profile at the mid-point of the test chamber.

To accommodate hydrogen testing, numerous modifications were made to the standard CS100 setup, including a dual enclosure that was constantly purged with nitrogen gas and encompassed the CS100 and most of the electrical equipment. A thorough description of the design and modifications to CS100, along with other saftey-realted topics required to perform testing with flammable gases can be found in reference 11. Figure 2 presents the CS100 during an LN_2 filling operation, the cold-mass removed from the vacuum chamber (chamber is in the background right) with the outer heater sleeve visible, and the radial temperature rake assembly.

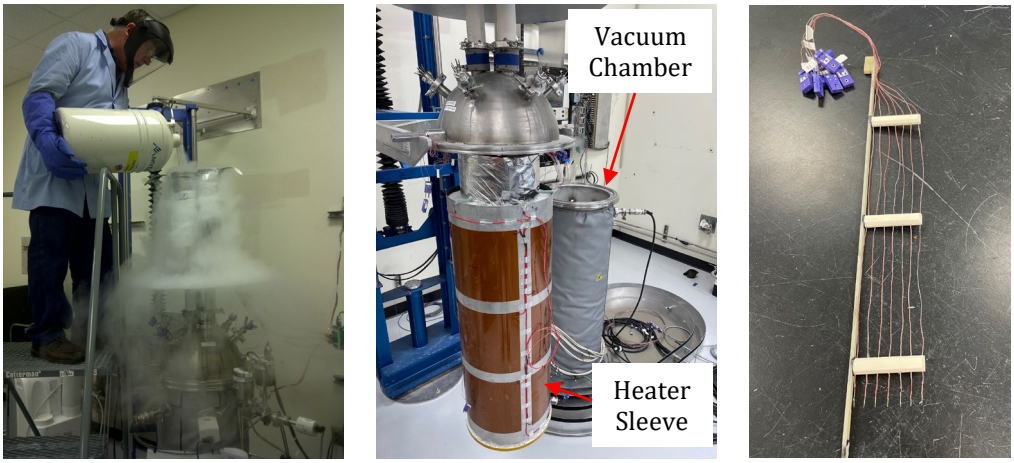

Figure 2. CS100 During LN_2 Fill Procedure (left); Cold-Mass Assembly Suspended from Vacuum Lid, with Heater Sleeve Visible (middle); Radial Temperature Rake Assembly (right)

3. Bulk-Fill Insulation Test Specimens

Three different samples were tested as part of the campaign: two different grades of perlite sourced from Silbrico Corporation—low density, Ryolex 3-S type, with an average bulk density of 49.1 kg/m^3; and high density, Ryolex 39 type, with an average bulk density of 123.3 kg/m^3—and K1 type glass bubbles from 3M Corporation, with a bulk density of 75 kg/m^3. Perlite is an expanded volcanic rock of varying particle sizes, ranging from <0.149 mm to 0.595 mm for Ryolex 39, and <0.149 mm to 1.19 mm for Ryolex 3-S. Glass bubbles are hollow glass microspheres, with an average diameter of 65 microns, and a particle size range from 30 to 115 microns.

Higher density perlite has been the insulation of choice historically for large, vacuum-insulated, field erected LH_2 tanks [12], with glass bubbles undergoing extensive testing at the CTL over the last 15 years for its use in LH_2 applications [13-15], which led to their implementation in the new tank at KSC [3]. Low density perlite is typically used for warmer boiling point cryogens such as liquid oxygen or LNG, in a non-vacuum configuration paired with background gases such as nitrogen. Although not used for LH_2 tanks, low density perlite was included as part of this examination for sake of completeness; to round-out the common bulk-fill insulation options.

Preparation and installation of the samples into CS100 involved thorough mixing of the powders in a large bin to homogenize the particle distribution, followed by filling by hand via a scoop-and-pour method from the top of the cold-mass assembly. As minimal dynamic loads are present during operation of CS100, it is assumed that negligible settling occurred during testing, and that the bulk densities remained uniform, and at the aforementioned values.

Following installation, the samples were subjected to a “bake-out” period to remove any trapped moisture. Samples were heated to roughly 350 K under active vacuum pumping for 3 to 5 days until the pressure dropped well below 1 torr (typically 10 to 100 millitorr), indicating that the majority of the moisture had been evacuated. Specimens remained under vacuum or dry background gas purge throughout the remainder of the test campaign, only being exposed to the ambient environment during sample change-out procedures.

Due to project constraints, only a single test campaign was conducted for each of the three insulation specimens, and consisted of one round each using nitrogen, helium, and hydrogen background gases, from high vacuum (<10^{-3} torr) to ambient (760 torr). Each pressure target ≥10 torr was tested multiple times in helium and hydrogen due to the relatively short duration (<1 hour). For those instances, the data presented are the statistical averages over all tests. For all other cases the test duration spanned multiple hours to days at high vacuum, hence yielded stable results and required only a single test.

4. CS100 Testing Limitations

For reasons that are not well understood at this time, long-duration steady-state conditions were difficult or impossible to achieve in some cases when testing at pressures ≥10 torr in helium and hydrogen. The boiloff flow rarely stabilized at a constant value for more than roughly 10 minutes for the high-density perlite, and struggled in this range as well for the low-density perlite. Glass bubbles however, yielded much more consistent steady-state tests across all pressures and background gases. This short period of stability always followed an LN_2 refill operation, when the test chamber pressure and flow rate climbed after installing the flow meter tube, briefly leveling off, and then decreasing at a relatively constant rate for the remainder of the test. This behavior is in stark contrast to a "normal" steady-state test, where the boiloff flow rate and pressure remain stable over hours, or even days when testing very high performance MLI.

For these pseudo-steady-state tests, because the duration was very short, the k_e and q values presented in the following sections are denoted differently than for the normal tests: with open markers instead of closed ones. For these cases the uncertainty could be slightly larger than the 3.3% for k_e and 3.2% for q [10] associated with a typical CS100 measurement, but by how much is unknown at this time.

5. Test Results – Effective Thermal Conductivity and Heat Flux

Figures 3 and 4 present the heat flux and effective thermal conductivity results for each test case over the entire vacuum pressure range. Orange curves represent hydrogen background tests, green correspond to helium, and blue nitrogen. Each insulation specimen is represented by a different marker, and each marker corresponds to an individual test. Solid markers denote steady-state tests, and open markers are reserved for pseudo-steady-state tests. Nominal warm and cold boundary conditions for each test case are 293 K and 78 K respectively. Heat flux values are based on the log-mean area between the test chamber and heater sleeve (0.4347 m^2).

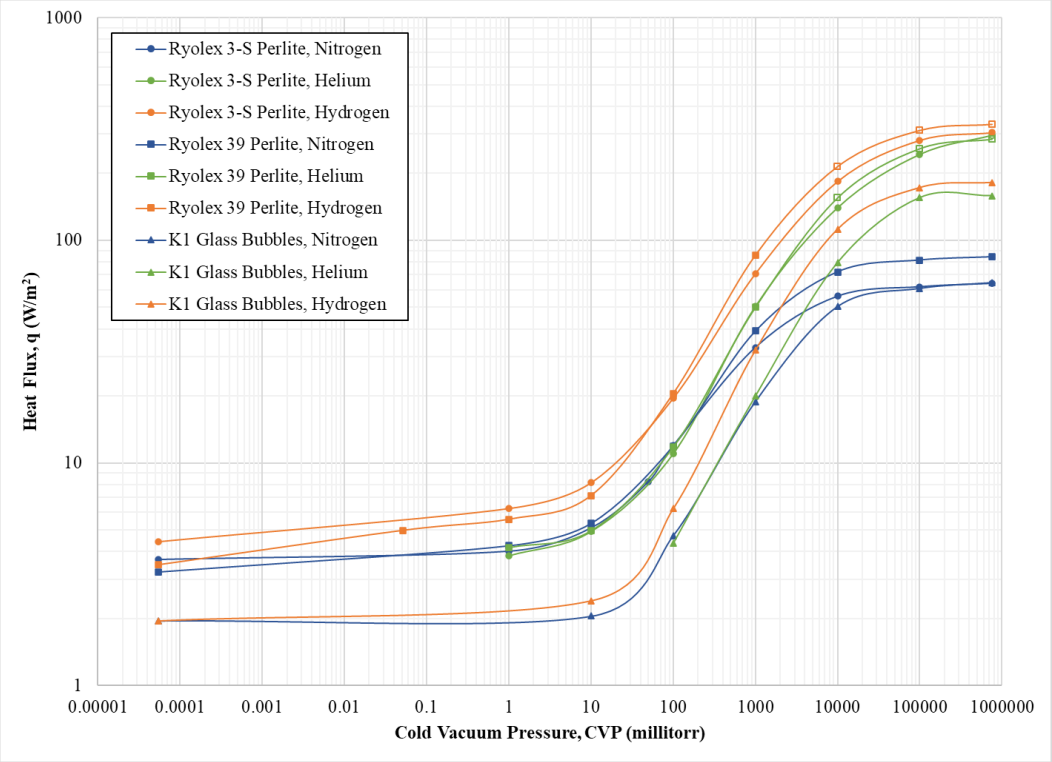

Figure 3. Heat Flux Results

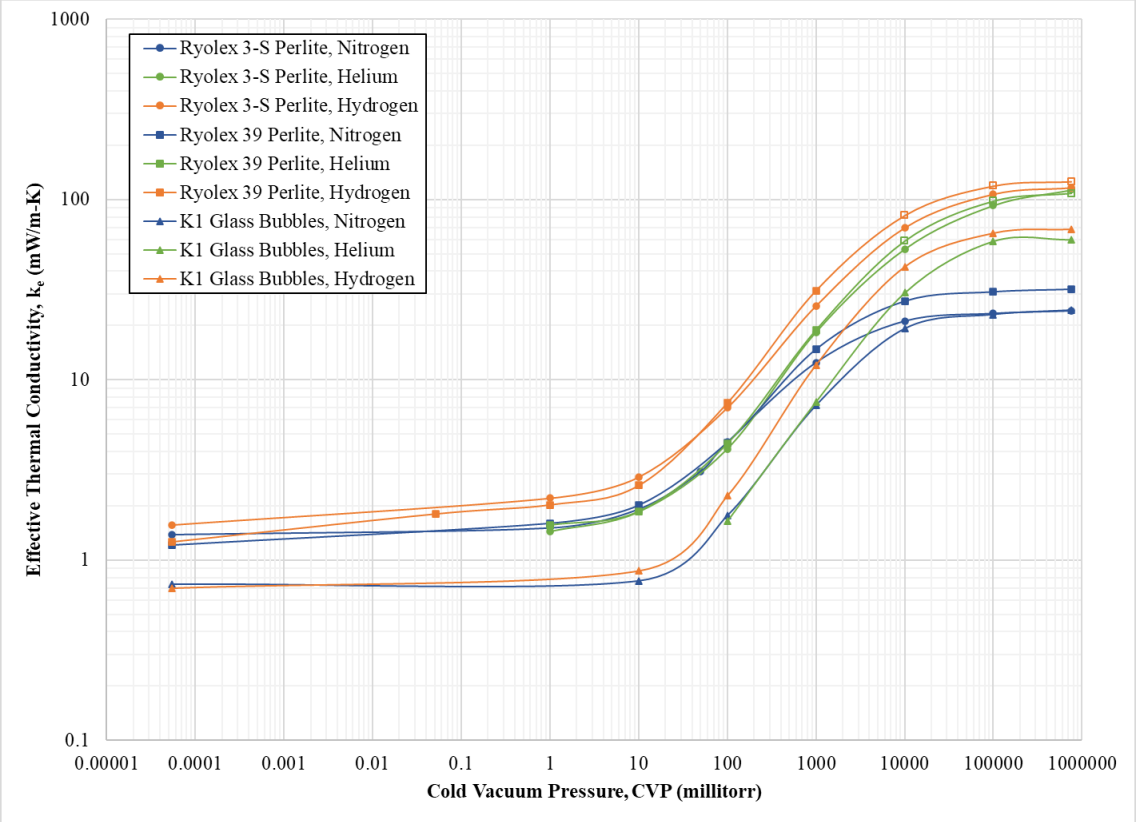

Figure 4. Variation of Effective Thermal Conductivity vs. Cold Vacuum Pressure

5.1 Discussion of k_e and q Test Results

Figures 3 and 4 reveal that at pressures above 1 torr the insulation performance is markedly worse for both helium and hydrogen background gases compared to nitrogen, with both gases yielding similar k_e values at 760 torr (note: the inflection in the curve for glass bubbles in helium between 100 torr and 760 torr is due to curve-fitting; k_e and q values are slightly higher at 760 torr). This result was expected; however, the magnitude of the increase in k_e above nitrogen is not simply proportional to the thermal conductivity of the gases as intuition might suggest. At 760 torr, and a mean temperature of 186 K (the average between the nominal warm and cold boundary temperatures), the ratio of the gas thermal conductivities is 6.6 for helium vs. nitrogen, and 7.3 for hydrogen vs. nitrogen (evaluated using RefProp version 10). Whereas the ratio of k_e for the high-density perlite (Ryolex 39) at the same conditions was only 3.4 and 4.0 for helium and hydrogen vs. nitrogen respectively. Low-density perlite (Ryolex 3-S) was higher at 4.3 and 5.8, and glass bubbles were lower at 2.5 and 2.8.

Another feature that stands out is that below pressures of roughly 1 torr the three insulations perform essentially equivalently for helium and nitrogen, but not for hydrogen. For hydrogen tests, the heat loads remained higher across almost the entire vacuum range; this was especially so for the perlite samples, even at very low pressures. An explanation for this is not readily apparent, but may be attributable to the higher molecular speed of hydrogen molecules compared to helium (1.4 times at 186 K), which could allow the former to transport heat more efficiently through the material at low pressures.

Other notable features from figures 3 and 4 are that the low-density perlite and glass bubbles show virtually identical performances in nitrogen >1 torr, but that is not the case for the other gases. Also, at high vacuum, high-density perlite performs slightly better than low-density perlite, while glass bubbles outperform both by a factor of 2 roughly.

6. Test Results – Thermal Profiles

Figure 5 presents the radial thermal profile for the high-density perlite sample (Ryolex 39). Low-density perlite and glass bubbles showed similar trends, hence are not included here.

The most notable feature in figure 5 is the large ΔT within the first 10 mm layer at the cold side. This existed for each sample tested, and became more pronounced with a decrease in vacuum pressure. At high vacuum, each sample saw a ΔT of roughly 123 K within the first layer—about 57% of the total ΔT across the 80.8 mm insulation thickness. Within the remaining layers the profiles followed a more predictable trend up to the warm boundary temperature. This behavior seems to suggest that the bulk of the insulation performance stemmed from the region closest to the cold-mass. Alternatively, the trends may be the result of the rake design itself. Since the radial foam standoffs that positioned the thermocouples were anchored to the warmer side of the sample, heat may have leaked through the lower standoff and influenced the thermocouples. However, two different rake designs were tested with similar outcomes, and a simple analysis of the current design suggested that heat leak though the standoffs was negligible. Understanding this large ΔT will be a specific topic of interest for future examinations.

Two additional points to note in figure 5: The slight dip in values at 30.3 mm is believed to be caused by the thermocouple at that location becoming bent slightly toward the cold side during installation of one of the samples; and the slightly higher warm boundary temperature for hydrogen tests at low pressures was a result of the elevated temperature inside the purged enclosure around the CS100. With equipment such as the vacuum pump continuously running inside the enclosure the environmental temperature increases, which warms the vacuum chamber above the desired warm boundary of 293 K and influences the inner heater sleeve—which is where the warm boundary temperature is defined/measured. This only applies to hydrogen, as the enclosure was only employed for flammable background gases. For other tests the enclosure was open, and the facility HVAC system maintained the vacuum chamber temperature close to 293 K.

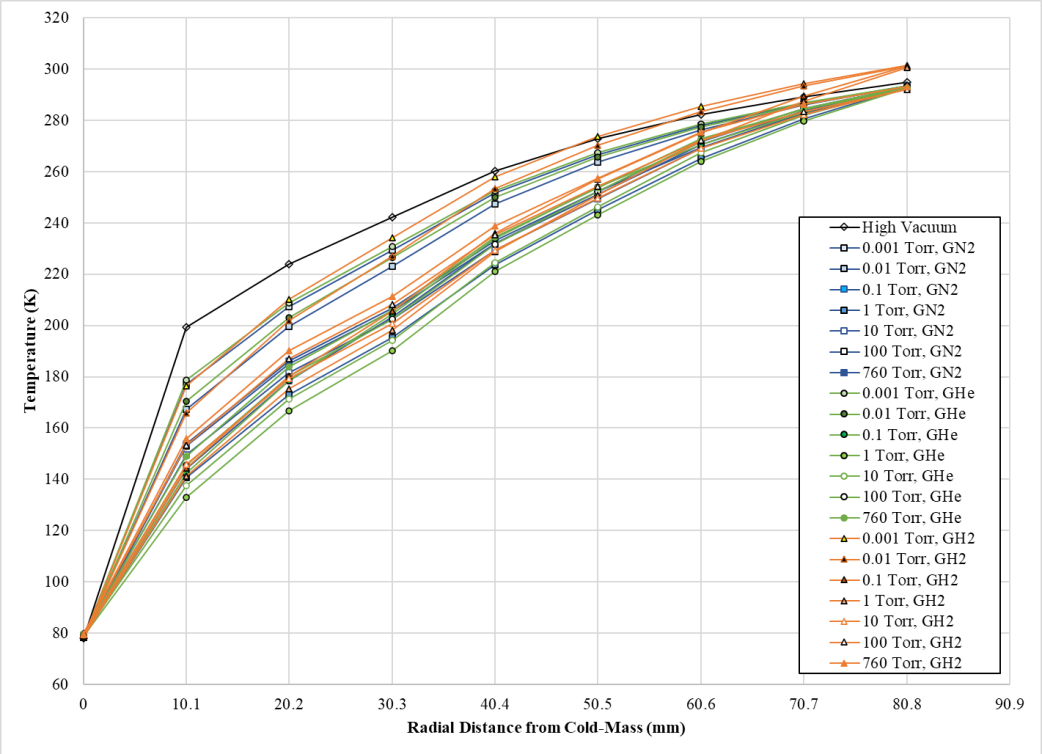

Figure 5. Radial Thermal Profile, Ryolex 39 Perlite

7. Conclusion

In support of future mega-scale liquid hydrogen storage tank development, the Cryogenics Test Laboratory at NASA Kennedy Space Center has recently executed a test campaign to characterize the thermal performance of common bulk-fill insulation materials in helium and hydrogen background gases. Using the ASTM standard CS100 instrument, a vertical-cylindrical liquid nitrogen boiloff calorimeter, low- and high-density perlite, and glass bubble materials were tested across the entire vacuum pressure range (i.e. $\sim 10^{-6}$ torr to 760 torr), at a thickness of 80.8 mm, and nominal warm and cold boundary temperatures of 293 K and 78 K respectively.

Results of this testing campaign were presented in terms of effective thermal conductivity and heat flux for each insulation/gas/vacuum combination, including nitrogen as a baseline, and verified an expected decrease in performance for the lighter helium and hydrogen gases versus nitrogen, though less than would be expected when compared to the increase in thermal conductivity of the individual gases.

Representative radial thermal profiles over the entire set of tests for one of the insulation samples was also presented, and revealed a large ΔT across the first 10.1 mm thick insulation layer, closet to the cold side, that increased with decreasing pressure. At its maximum, this ΔT was up to 57% of the total temperature difference across the sample.

Acknowledgments

This work was funded through the U.S. DOE's Office of Energy Efficiency and Renewable Energy (EERE) under the Hydrogen and Fuel Cell Technologies Office, H2@Scale Initiative, Award Number DE-EE0009387, led by Shell International Exploration & Production Inc.

References

[1] Simanullang, M., Liquid hydrogen storage and insulation materials for liquid hydrogen storage tanks: Trends and challenges, 2025, *International Journal of Hydrogen Energy*, **140**, Pages 881-888
[2] Krenn, A., and Desenberg, D., Return to service of a liquid hydrogen storage sphere, 2020 *IOP Conf. Ser.: Mater. Sci. Eng.* **755** 012023
[3] Fesmire, J E, et al., Energy efficient large-scale storage of liquid hydrogen, 2022 *IOP Conf. Ser.:* **1240** 012088
[4] Ishimoto, Y., et al., Large-scale production and transport of hydrogen from Norway to Europe and Japan: Value chain analysis and comparison of liquid hydrogen and ammonia as energy carriers, 2020, *International Journal of Hydrogen Energy*, Vol. **45**, Issue 58, Pages 32865-32883,
[5] Jungwoog K. et al., Technical feasibility of large-scale transportable liquid hydrogen export terminal, *International Journal of Hydrogen Energy*, Vol. **66**, 2024, Pages 499-511,
[6] van Doorne, C., et al., Unlocking the Potential of Liquid Hydrogen Supply Chains, 2025, Proceedings of Gastech 2025 Conference, Milan, Italy
[7] Anderson, S.T., Economics, Helium, and the U.S. Federal Helium Reserve: Summary and Outlook, 2018, *Nat Resour Res* **27**, Pages 455–477
[8] Zang, K., Rajagiri, N., and Damle-Mogri, S., Hydrogen: A small but mighty molecule with a critical net-zero role to play, Shell TechXplorer Digest: Special Edition 2024, pages 64-69,
[9] ASTM C1774 Standard Guide for Thermal Performance Testing of Cryogenic Insulation Systems, 2019, (West Conshohocken, PA: ASTM International)
[10] Fesmire, J E, et al., Cylindrical boiloff calorimeters for testing of thermal insulation systems, 2015 *IOP Conf. Ser.: Mater. Sci. Eng*. **101** 012056 2015
[11] Swanger, A M., et al., A Boiloff Calorimetry Test Configuration for the Characterization of Thermal Insulation Systems in Flammable Background Gases, 2024, Proceedings of the 29th International Cryogenic Engineering Conference, Geneva, Switzerland
[12] Swanger A M., et al., Vacuum Pump-Down of the Annular Insulation Space for Large Field-Erected Liquid Hydrogen Storage Tanks, 2024, *IOP Conf. Ser.: Mater. Sci. Eng.* **1301** 012066
[13] Sass, J E. et al., THERMAL PERFORMANCE COMPARISON OF GLASS MICROSPHERE AND PERLITE INSULATION SYSTEMS FOR LIQUID HYDROGEN STORAGE TANKS, 2008, *AIP Conf. Proc*. **985**, Pages 1375–1382
[14] Sass, J P. et al., GLASS BUBBLES INSULATION FOR LIQUID HYDROGEN STORAGE TANKS, 2010, *AIP Conf. Proc.* **1218**, Pages 772–779
[15] Fesmire, J E., et al., COST-EFFICIENT STORAGE OF CROGENS, 2008, *AIP Conf. Proc.* **985**, Pages 1383–1391